

Three-Photon Absorption in Nanostructure Wide-Band Gap Semiconductor ZnO Using Femtosecond Laser

Abdulla M. Suhail (Corresponding author)

Associate Professor Department of physics, College of science
University of Baghdad, Baghdad, Iraq
Tel: 964-770-871-0350 E-mail: Abdulla_shl@yahoo.com

Hani J. Kbashi

Department of physics, College of science
University of Baghdad, Baghdad, Iraq
Tel: 964-790-125-9537 E-mail: hani_saka@yahoo.com

Raied K. Jamal

Department of physics, College of science
University of Baghdad, Baghdad, Iraq
Tel: 964-770-080-3973 E-mail: raiedkamel@yahoo.com

Received: July 12, 2011

Accepted: September 8, 2011

Published: December 1, 2011

doi:10.5539/mas.v5n6p199

URL: <http://dx.doi.org/10.5539/mas.v5n6p199>

Abstract

The three-photon absorption (3PA) in nanostructure wide-band gap ZnO semiconductor material is observed under high intensity femtosecond Titanium-Sapphire laser of 800 nm wavelength excitation. The ZnO nanofilms were prepared by chemical spray pyrolysis technique with substrate temperature of 370 °C. The optical properties concerning the absorption, transmission, and the photoluminescence spectra are studied for the prepared nanofilms. The structure of the ZnO nanofilm was tested with the X-Ray diffraction and it was found to be a polycrystalline with recognized peaks oriented in (002), (101), and (100). The measured nonlinear absorption coefficient was found to be about $0.062 \text{ cm}^3/\text{Gwatt}^2$, which is about ten time higher than the bulk value. The observation of 3PA under the influence of intense laser radiation was attributed to the two-photon absorption followed by free carrier absorption. The fully computerized z-scan system was used to measure the nonlinear coefficients from the Gaussian fit of the transmitted laser incident. The observation of the three-photon absorption under high intensity in nanocrystalline material attributed to the resonance between the $3h\nu_{sph}$ and $h\nu_{flu}$ which is simply achieved in nanostructure.

Keywords: Multiphoton processes, ZnO nanocrystalline, Nonlinear optics, Three photon absorption

1. Introduction

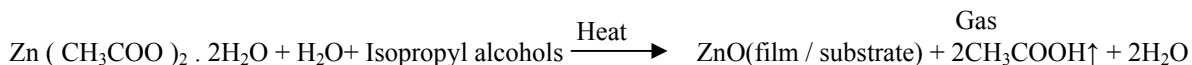
The ZnO nanostructures have many applications in gas sensors, UV detectors and solar cells Yanwu et al (2006), K. Ramanathan et al (2005), Crissy et al (2008). This material has some additional advantages compared to other large band-gap semiconductors; for example, its large exciton binding energy (about 60 meV) which is three times the binding energies of ZnSe and GaN Hua et al (2008). This allows a stable exciton distribution and achieves efficient excitonic emission at room temperature. The optical and electrical properties of ZnO nanostructures are studied at different preparation techniques and at different substrate materials Sato et al (2005), Shubra et al (2007). The pumping of ZnO crystalline film with near-infrared femtosecond radiation pulses, enhances the nonlinear interaction between the ultrahigh intensity applied optical field and the ZnO nanostructures U. Ozgura et al (2005), Ja-Hon et al (2005). The nonlinear interaction leads to the simultaneous absorption of two or more photons of subbandgap energy. The absorption is through a virtual-states that assists the inter band transitions. This transition produces electron-hole pairs in the excited states and, subsequently, the

band-edge emission via their radiative recombination Sean et al (2007). The two photon absorption (2PA) in semiconductor nanocrystals (NCs) has been widely investigated E. W. et al (1993), Ja-Hon et al (2005), while the research effort on their three – photon absorption (3PA) is limited Jun et al (2006). The three photon absorption was observed in ZnO and ZnS crystals when pump with lasers of ultra excitation irradiance which was more than 40 GW/cm² Bing et al (2008), Shaul et al (2008), A. Penzkofer et al (1976), E. Mazur et al (2010).

In this work the three photon absorption in ZnO nanostructure illuminated by intensity 79GW/cm² Ti-Sapphire laser is observed. The work concentrates on the effect of the nanostructure on the nonlinear parameters through the studying of the 3PA coefficient and the laser threshold pumping power. Simple mathematical relations are developed to describe the dependence of the fluorescent emission on the pumping laser intensity. The three photon absorption coefficient was calculated from the experimental measurements.

2. Experimental work

The ZnO nanofilm was prepared by chemical spray pyrolysis technique. The film was deposited on quartz substrates heated to 370 °C. The spray solution is prepared by mixing Zinc acetate (Zn (CH₃COO)₂·2H₂O), isopropyl alcohol with purity 95 % and distilled water in a volume ratio 3 : 1 at 0.2 M. The above mixture solution was placed in the flask of the atomizer and spread by controlled nitrogen gas flow on the heated substrates. The chemical spray pyrolysis experimental setup is similar to the standard unit fully described by M. Islam et.al (2009). The spraying time was controlled by adjustable a solenoid valve. The heated substrate was left for 12 sec after each spraying run to give time for the deposited ZnO layer to be dry. In order to get a film of proper thickness many layers deposited of ZnO are required. The optimum experimental conditions for obtaining homogeneous ZnO thin film at 370 °C are determined by the spraying time, the drying time and the flashing gas pressure. The schematic representation of the spray system is given in Figure 1. The possible reaction of the spray chemical on the heated substrate is yielding for the following reaction:



During the chemical reaction, gas and water vapor is obtained from this reaction due to the high temperature of the substrate. At the end of the reaction a white precipitates remain from the reaction as a nanofilm of ZnO. The topography study of the prepared nanofilm surface was carried out using Scanning Electron Microscopy (SEM) type ULTRA 55 with different magnification; as shown in Figure 2. The X-ray diffraction (XRD) pattern of ZnO nanofilm was recorded by XRD 2000. The X-Ray diffractometer use copper tube radiation line of wavelength 1.54 Å in 2θ range from 20° to 60°. The scanning rate was 1deg/min.

The UV-VIS absorption and transmission spectra of the sample were recorded by Hitachi U-4100 spectrometer covering the spectral range (200-1100nm). The photoluminescence spectrum (PL) was studied using SL1174 spectrophotometer in the range 300-900 nm.

The nonlinear absorption study at the near resonant regime was carried out using a fully computerized single beam femtosecond z-scan technique. The z-scan setting is illustrated by schematic diagram shown in Figure 3. A femtosecond laser of pulse duration 60 fs and of average power 6.7 mW was used as a laser source. The pulse duration was measured by autocorrelation system and the energy was measured by pyroelectric energy prob model type (PDA36A), covering the rang 350-1100 nm from THORLABS. The beam profile was adjusted by spatial filter leading to spatial intensity profile near Gaussian with beam quality of M² ≈1.24. The laser beam was focused by a lens of 15 cm focal length to produce a waist of 22.5 μm. The sample was translated along the beam axis (z-axis) through the Rayleigh distance 2000 μm.

3. Results and discussion:

The topography study of the prepared film shows the formations of the ZnO nanostructure and the film thickness was around 900 nm. The Figure showed Nanocrystals of size (50-100) nm. The micrography revealed that the particles were nearly spherical, which were regroup in the form of the flower like cluster. The XRD pattern of a ZnO nanofilm prepared with 900nm thickness is illustrated in Figure 4. The spectrum indicates that the ZnO film is a polycrystalline structure. The grains are highly oriented along the (002) direction implying that the crystal orientation is mostly along the c-axis perpendicular to the substrate surface. The spectrum through 2θ=20° to 2θ=60° indicates that the ZnO nanofilm is a polycrystalline structure. The observed values of the X-Ray diffraction peaks are compared with American Society for Testing and Materials (ASTM) data for hexagonal

Zinc Oxide. The Figure shows broad peaks which give evidence of the nanostructure formation. Using the width of (002) peak which appears at angle 34.38° on 2θ scale in Scherrer's formula A. Patterson (1939):

$$d = 0.94 \lambda / \beta \cos\theta \quad (1)$$

Where d is the average crystalline grain size, λ is the wavelength, β represents the full width at half maximum (FWHM) in radian and θ is the Bragg diffraction angle in degree, the size of the formed nanoparticles was found to be about 33 nm, this value is very close to the value obtained by SEM. Using the width of (110) peak which appears at angle 56.58° on 2θ scale the size of the formed nanoparticles was found to be about 20 nm.

The optical properties of ZnO films which were prepared on quartz substrates have been studied in this work. The absorption, transmission, and the photoluminescence PL Spectra of the ZnO film in the spectral range (300-800) nm are shown in Figures 5, 6 and 8 respectively. The absorption spectrum shows low absorbance in the visible and infrared regions; however, the absorption in the ultraviolet region is high. Referring to the data extracted from the absorption spectrum in Figure 5, the absorption coefficient (α) was calculated as a function of wavelength. Assuming allowed transition; the dependence of $(\alpha h\nu)^2$ on $(h\nu)$ is plotted as in Figure 7. The extrapolation of the linear part of the plot $(\alpha h\nu)^2 = 0$, gives rise on estimation of the energy gap value of the prepared ZnO nanofilm. The value of the energy gap was found to be about 3.3eV. This value was in a good agreement with values mentioned by other works Q. G. Al-zaidi et al (2009). The optical transmittance spectrum of the ZnO film is shown in Figure 6. It can be noticed from this Figure that the transmittance is high in the visible and infrared regions.

The PL spectrum of the ZnO film illuminated by 320 nm UV line is shown in Figure 8. The spectrum displays two major luminance peaks at 380 nm and around 556 nm. The first peak is due to the energy gap transmission which corresponds to 3.28 eV. The second peak is due to the excitonic emission; and it is in a good agreement with the results measured by many other authors K. Yim et al (2006), C. Xu et al (2008). The broad green emission peak that is dominated at 556 nm (≈ 2.23 eV) is a good evidence for the exciton formation in ZnO with a binding energy of 60meV. The high binding energy enables the finding of the exciton at room temperature. The intensity at the 556 nm peak is higher than that found around 380nm peak. This is because the band-to-band transition was quenched by the defect states. The same behavior was observed by Wang et.al (2008). The quenching of the band-to-band transition by the surface states was observed in CdS nanocrystalline samples illuminated by 320 nm UV line A. M. Suhail (2010).

The morphology of the ZnO film surface was imaged by Atomic Force Microscope (AFM), model ULTRA objective and illustrated in Figure 9. The Figure shows the formation of the nanostructures which helps in lowering the threshold laser power required to induced the nonlinear effect in the ZnO material. The surface roughness may attribute to the clustering of the grains in the films prepared under high ambient pressure Antaryami et al (2008), A. Mitra et al (2001), Anirban et al (2001).

The z-scan transition curve at 79 GW/cm² excitation intensity is recorded for the nanoparticles ZnO nanofilm and it shown in Figure 10. The normalized energy transmittance for 3PA of the open aperture z-scan is given by R. L. Sutherland et al (2003):

$$T(z) = \frac{1}{\pi^{1/2} p_o} \int_{-\infty}^{\infty} \ln \{ [1 + p_o^2 \exp(-2x^2)]^{1/2} + p_o \exp(-x^2) \} dx \quad (2)$$

Where $p_o = (2\gamma I_o^2 L'_{eff})^{1/2}$, $I_o = I_{oo} / (1 + z^2 / z_o^2)$ is the excitation intensity at the position z , $z_o = \pi \omega_0^2 / \lambda$ where z_o is the Rayleigh range, ω_0 is the minimum beam waist at focal point ($z=0$), λ is the laser free-space wavelength, $L'_{eff} = [1 - \exp(-2\alpha oL)] / 2\alpha o$ is the effective sample length for 3PA processes; L is the sample length and αo is the linear absorption coefficient. The open aperture z-scan graphs are always normalized to linear transmittance i.e., transmittance at large values of $|z|$. The 3PA coefficient can be extracted from the best fit between equation (2) and the experiment (OA) Z-scan curve. If $P_o < 1$ equation (2) can be expanded in a Taylor series as:

$$T = \sum_{m=1}^{\infty} (-1)^{m-1} \frac{p_o^{2m-2}}{(2m-1)! (2m-1)^{1/2}} \quad (3)$$

Furthermore, if the higher order terms are ignored, the transmission as a function of the incident intensity is given by R. L. Sutherland et al (2003):

$$T = 1 - \frac{\gamma I_o^2 L'_{eff}}{3^{3/2}} \quad (4)$$

The solid curve in Figure 10 is the best fit for equation (4). The equation (4) shows clearly that the depth of the absorption dip is linearly proportional to the 3PA coefficient γ , but the shape of the trace is primarily determined by the Rayleigh range of the focused Gaussian beam. The fitted value of γ is on the order of $0.062 \text{ cm}^3/\text{Gwatt}^2$. This value is ten times of magnitudes higher than the value observed with bulk ZnO sample. The natural logarithm of the (1-T) values are plotted as a function of natural logarithm of the incident intensity I_0 in Figure 11. The curve can be reasonably fitted with a straight line with slope of 1.99, this indicates that the 3PA was occurred in ZnO pumped by 800 nm laser source of 60 fs pulse duration as shown in Figure 11.

4. Conclusion

The three-photon absorption has been observed in ZnO nanocrystalline prepared by chemical method upon illuminating it by femtosecond Titanium-Sapphire laser. The fully computerized z-scan system was used to measure the nonlinear absorption coefficient of the prepared samples. The value of the measured nonlinear coefficient was found to be ten times higher than the bulk value. The enhancement of the nonlinear coefficient was attributed to the formation of the nanocrystallites of ZnO and to the existence of the exciton in the prepared nanofilm.

Acknowledgments

This work has been carried out in the physics Department, School of Engineering and Applied Sciences, Harvard University. The authors would like to thank Mazur Research Group in Harvard University for their help through this work. Thank also to Christopher C. Evans, Jonathan D. B. Bradley, and Eric Mazur for their interest, guide and useful discussion. We thank also the Ministry of Higher Education in the republic of Iraq for support this work.

References

- Anirban, M., & Thareja, R. K. (2001). Photoluminescence and ultraviolet laser emission from nanocrystalline ZnO thin films. *Journal of Applied Physics*, 89, 2025–2028. <http://dx.doi.org/10.1063/1.1342803>
- Antaryami, M., & Thareja, R. K. (2008). Photoluminescence study of ZnO nanowires grown by thermal evaporation on pulsed laser deposited ZnO buffer layer. *Journal of Applied Physics*, 104, 044906. <http://dx.doi.org/10.1063/1.2969908>
- Al-zaidi, Q. G., Suhail, A. M., Al-azawi, W. R. (2011). Palladium – doped ZnO thin film hydrogen gas sensor. *Applied Physics Research*, 3, 1, 89 – 99.
- Bentley, S. J., Anderson, C. V., & Doohar, J. P. (2007). Three-photon absorption for nanosecond excitation in cadmium selenide quantum dots. *Optical Engineering*, 46, 128003. <http://dx.doi.org/10.1117/1.2823156>
- Gu, B., He, J., Ji, W., & Wang, H. T. (2008). Three-photon absorption saturation in ZnO and ZnS crystals. *J. Applied Physics*, 103, 073105. <http://dx.doi.org/10.1063/1.2903576>
- He, J., Ji, W., & Mi, J. (2006). Three-photon absorption in water –soluble nS 18 nanocrystal. *Appl. Phys. Lett*, 88, 181114. <http://dx.doi.org/10.1063/1.2198823>
- Islam, M. R., & Podder, J. (2009). Optical properties of ZnO nanofiber thin film grown by spray pyrolysis of zinc acetate precursor. *Cryst. Res. Technol*, 44, 286-292. <http://dx.doi.org/10.1002/crat.200800326>
- Lin, J. H., Chen, Y. J., Lin, H. Y., & Hsieh, W. F. (2005). Two-photon resonance assisted huge nonlinear refraction and absorption in ZnO thin films Institute of Electro-Optical Engineering. *J. Appl. Phys*, 97, 033526. <http://dx.doi.org/10.1063/1.1848192>
- Li, H., Sang, J. P., Liu, C., Lu, H. B., & Cao, J. C. (2008). Microstructural study of MBE-grown ZnO film on GaN/sapphire (0001) substrate. *Cent. Eur. J. Phys*, 6, 638-642. <http://dx.doi.org/10.2478/s11534-008-0032-2>
- Mitra, A., Thareja, R. K., Ganesan, V., Gupta, A., Sahoo, P. K., Kulkarni, V. N. (2001). Synthesis and characterization of ZnO thin films for UV laser. *Applied Surface Science*, 174, 232-239. [http://dx.doi.org/10.1016/S0169-4332\(01\)00171-4](http://dx.doi.org/10.1016/S0169-4332(01)00171-4)
- Penzkofer, A., & Falkenstein, W. (1976). Three photon absorption and subsequent excited-state absorption in CdS. *optics communication*, 16, 247-250.
- Patterson, A. L. (1939). *Phys. Rev*, 56, 978. <http://dx.doi.org/10.1103/PhysRev.56.978>
- Rhodes, C. L., Lappi, S., Daniel, F., Sharadha, S., Genzer, J., & Stefan, F. (2008). Characterization of Monolayer Formation on Aluminum-Doped ZincOxide Thin Films. *American Chemical Society*.

- Suhail, A. M., Khalifa, M. J., Saeed, N. M., & Ibrahim, O. A. (2010). White light generation from CdS nanoparticles illuminated by UV-LED. *Eur. Phys. J. Appl. Phys*, 49, 30601. <http://dx.doi.org/10.1051/epjap/2010005>
- Sutherland, R. L., McLean, D. G., & Kirkpatrick, S. (2003). *Handbook of Nonlinear Optics*. Second Edition. Reserved and Expanded .New York, NY:Marcel Dekker.
- Sato,T., Suzuki, H., Kido, O., Kurmada, M., Kamitsuji, K., Kimura, Y., Kawaski, H., et al.(2005). Production of transition metal-doped ZnO nanoparticles by using RF plasma field. *J. Crystal Growth*, 275, 983-987. <http://dx.doi.org/10.1016/j.jcrysgro.2004.11.152>
- Shaul, P., Rotenberg, N., & Henry, M. V. D. (2008). Three photon absorption in silicon for 2300-3300nm. *Appl. Phys. Lett*, 93, 131102. <http://dx.doi.org/10.1063/1.2991446>
- Shubra, Singh, & Rao, M. S. R. (2007). Structure and Physical Properties of Undoped ZnO and Vanadium Doped ZnO films deposited by Pulsed Laser deposition. *J. nanoscience and nanotechnology*. 8, p1-3.
- Ü. Özgür, Alivov, Y. I., Liu, C., Teke, A., Reshchikov, M. A., Doğan, S., & Avrutin, V., et al. (2005). A comprehensive review of ZnO materials and devices. *J. Appl. Phys*, 98, 041301. <http://dx.doi.org/10.1063/1.1992666>
- Van Stryiand, E. W., Sheik-Bahae, M., Said, A. A., & Hagan, D. J. (1993). Characterization of nonlinear optical absorption and refraction. *Prog. Crystal Growth and Charact*, 27, 279-311. [http://dx.doi.org/10.1016/0960-8974\(93\)90026-Z](http://dx.doi.org/10.1016/0960-8974(93)90026-Z)
- Vivas, M. G., Shih, T., Voss, T., Mazur, E., & Mendonca, C. R. (2010). Nonlinear spectra of ZnO: reverse saturable, two- and three-photon absorption. *Opt. Express*, 18, 9628-9633. <http://dx.doi.org/10.1364/OE.18.009628>
- Wang, D. D. Yang, J. H., Yang, L. L., Zhang, Y. J., Lang, J. H., & Gao, M. (2008). Morphology and photoluminescence properties of ZnO nanostructures fabricated with different given time of Ar. *Cryst.Res. Technol*, 43, 1041-1045. <http://dx.doi.org/10.1002/crat.200800109>
- Xu, C. X., Zhu, G. P., Li, X., Yang, Y., Tan, S. T., Sun, X., Lincoln, W. C., et al. (2008). Growth and spectral analysis of ZnO nanotubes. *Journal of Applied Physics*, 103, 094303. <http://dx.doi.org/10.1063/1.2908189>
- Ramanathan, K., Keane, J., & Noufi, R. (2005). Properties of High- Efficiency CIGS Thin –Film Solar Cells. *NREL/CP*, 520, 37404.
- Yim, K., & Lee, C. (2006) Optical properties of Al-doped ZnO thin films deposited by two different sputtering methods. *Cryst.Res. Technol*, 41, 1198-1202. <http://dx.doi.org/10.1002/crat.200610749>
- Zhu, Y. W., Elim, H. L., Foo, Y. L., Yu, T., Liu, Y. J., Ji, W., Lee, J. Y., et al.(2006). Multiwalled Carbon Nanotubes Beaded with ZnO nanoparticles for Ultrafast Nonlinear Optical Switching. *Adv. Mate*, 18, 587-592. <http://dx.doi.org/10.1002/adma.200501918>

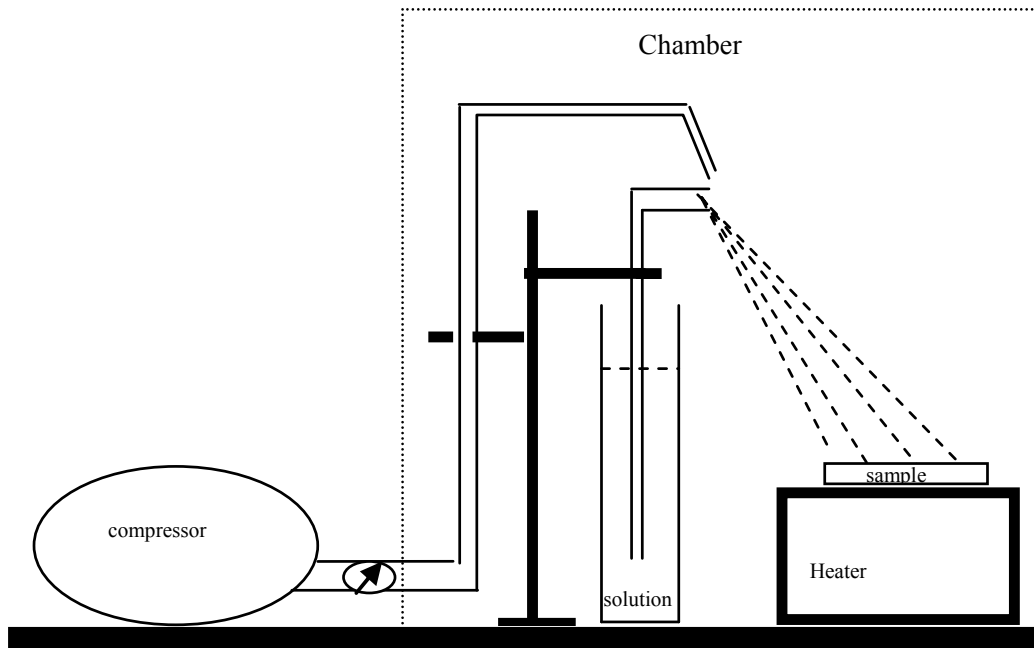


Figure 1. Schematic representation of the spray system

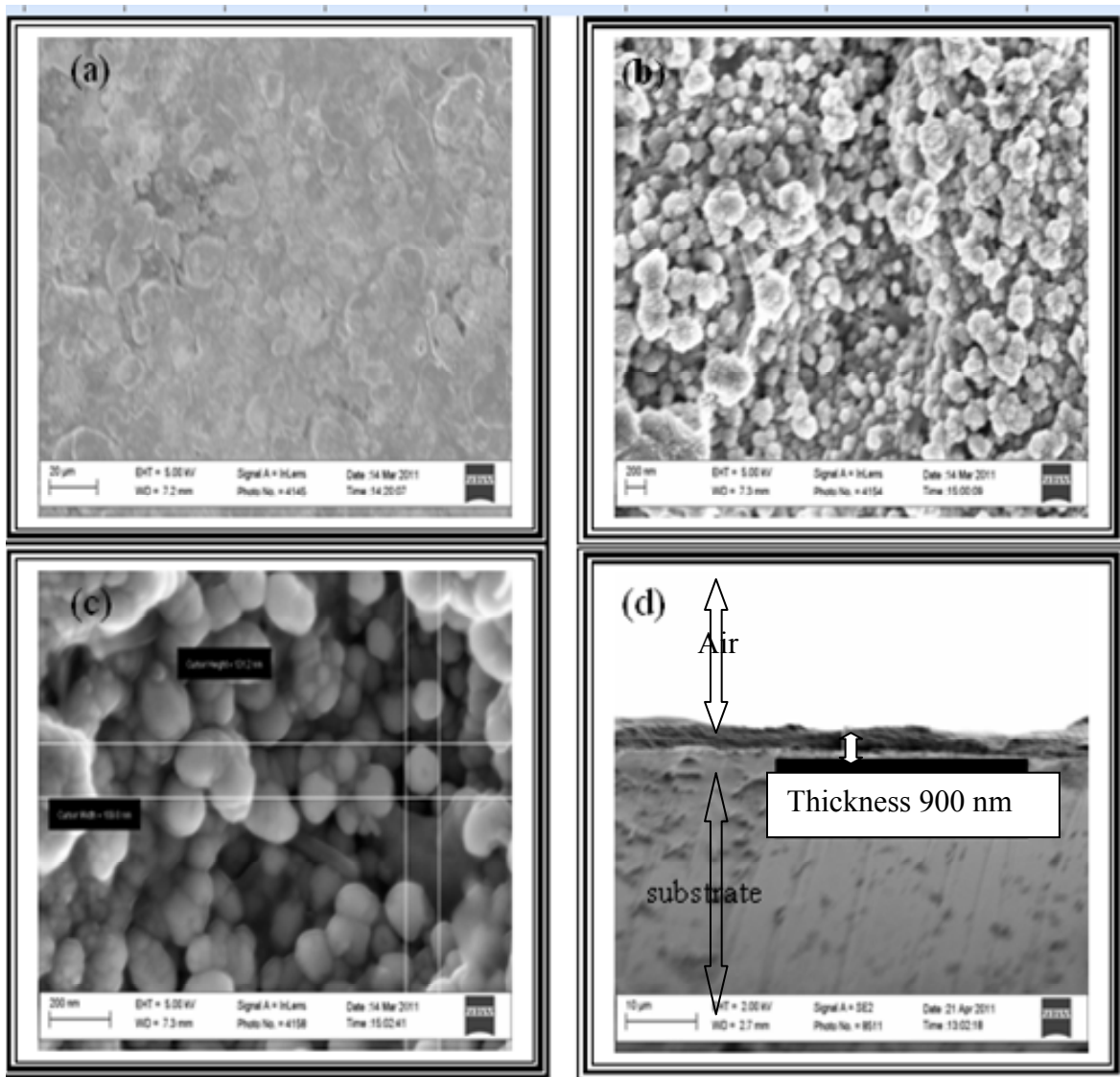


Figure 2. a,b,c represent SEM images of ZnO nanofilm at different magnification power and (d) for a sample thickness

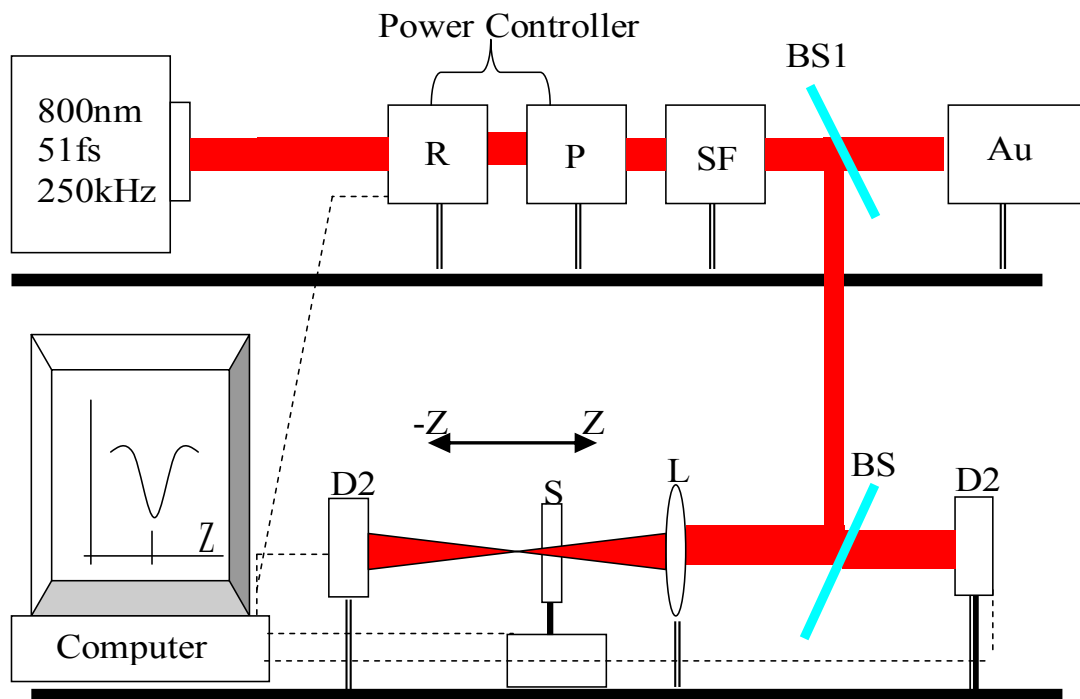


Figure 3. Schematic of the z-scan setup recording the nonlinear absorption. R-Rotator, P-Polarizer, SF-Spatial filter, BS1, BS2-Beam Splitter, Au-Autocorrelation, D1,D2-Dectors, L-Lens, S-Sample.

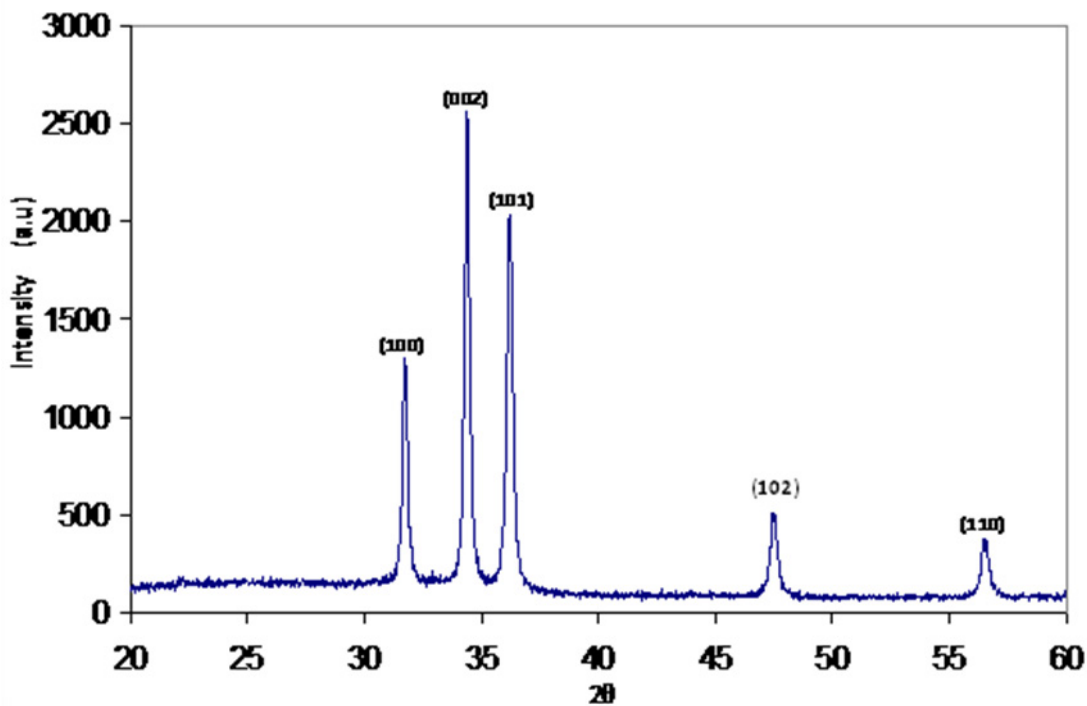


Figure 4. XRD pattern of ZnO nanofilm deposited on a glass substrate at 370 °C

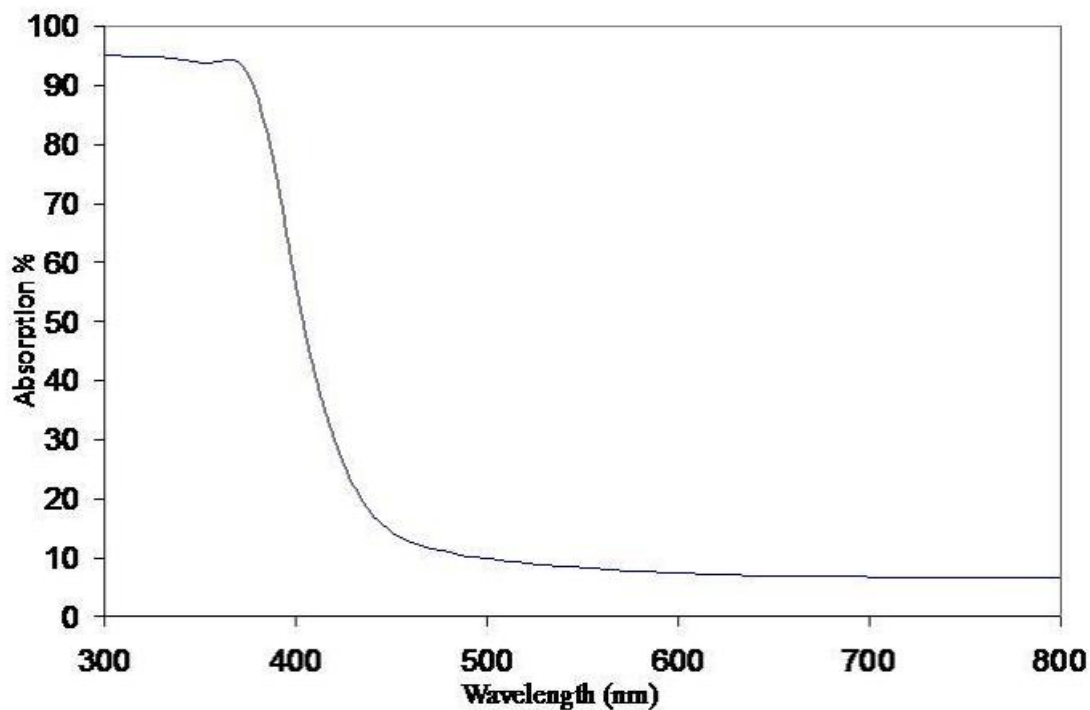


Figure 5. Optical absorption spectra of ZnO nanofilm

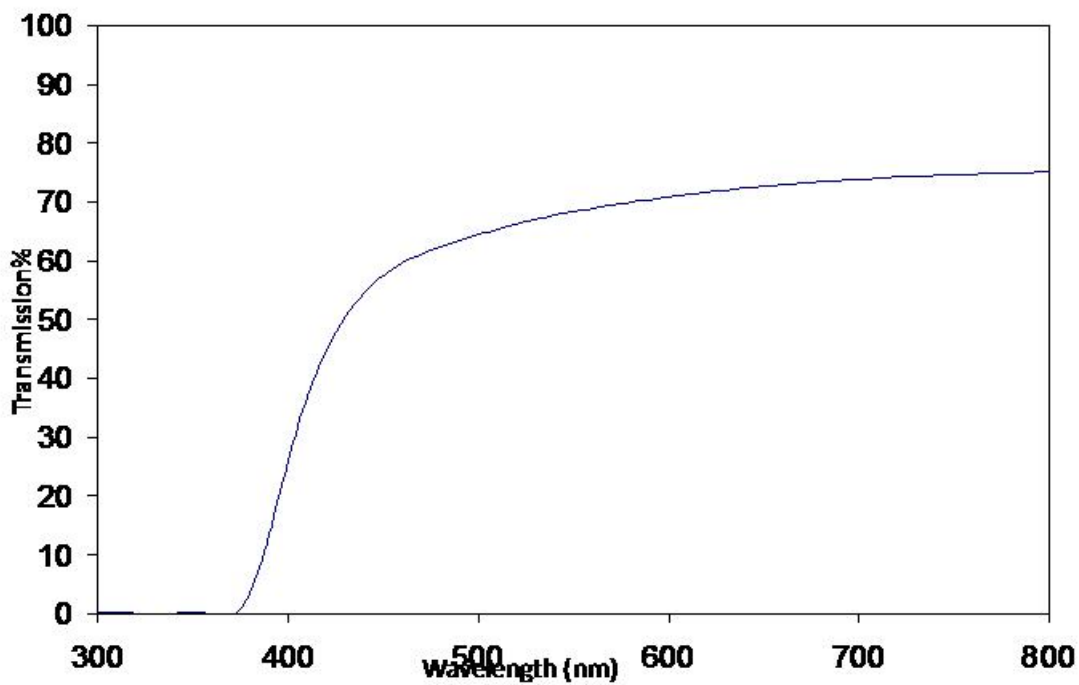


Figure 6. Optical transmission spectra of ZnO nanofilm

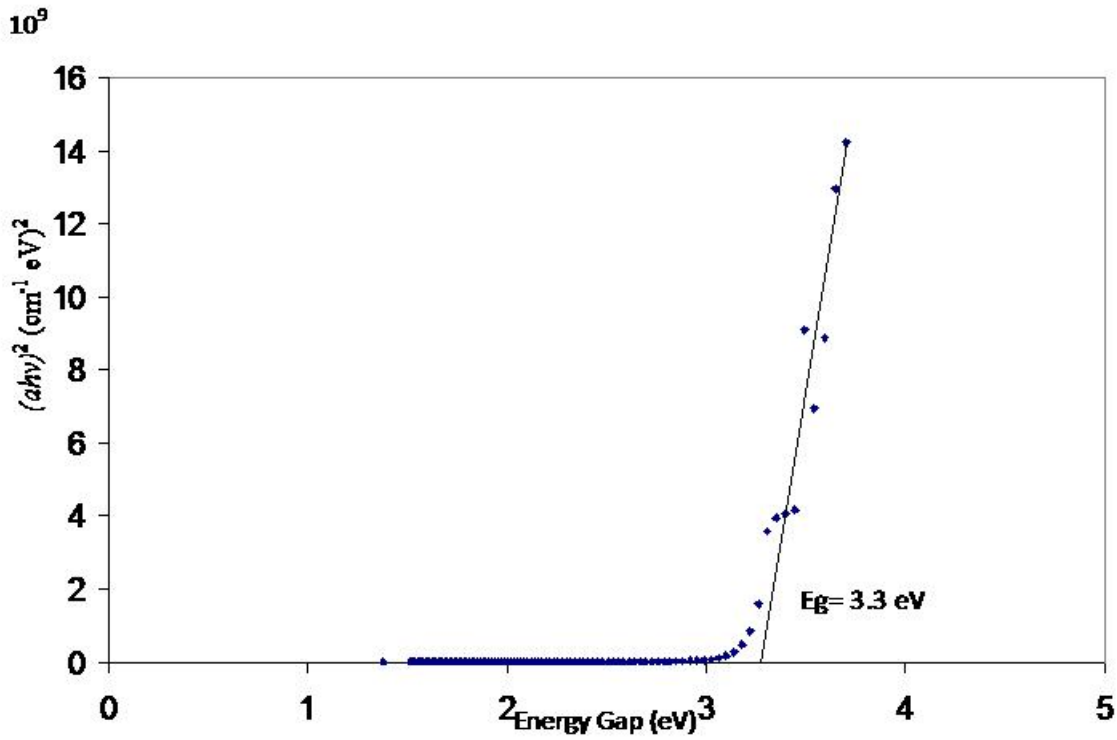


Figure 7. $(ah\nu)^2$ versus energy gap

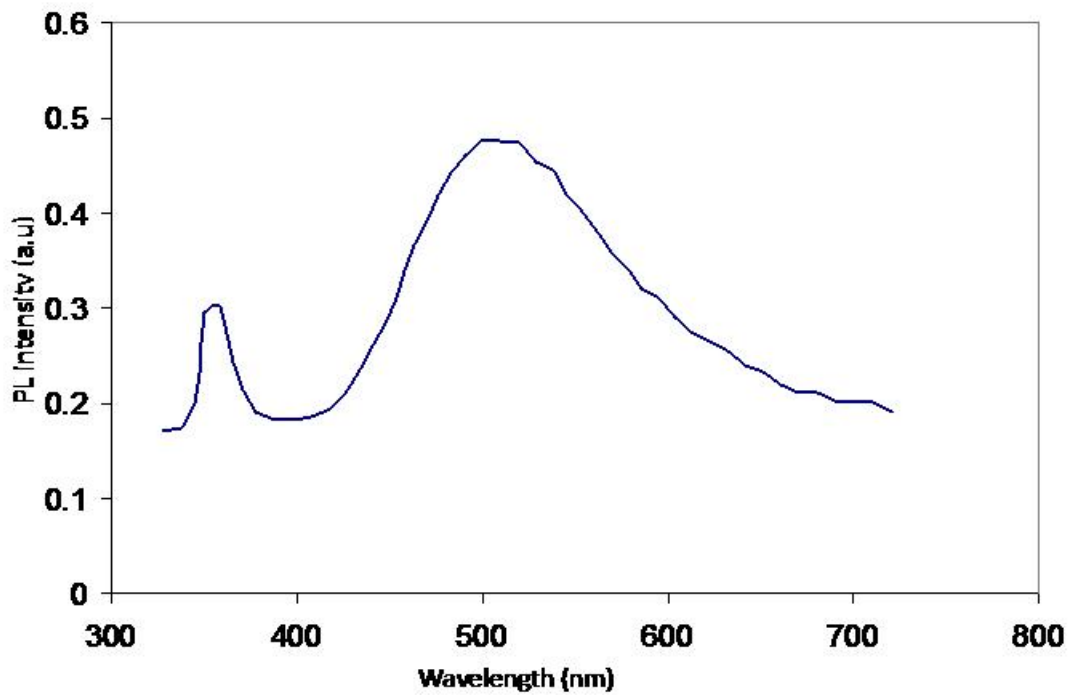


Figure 8. Photoluminescence emission spectrum of ZnO nanofilm

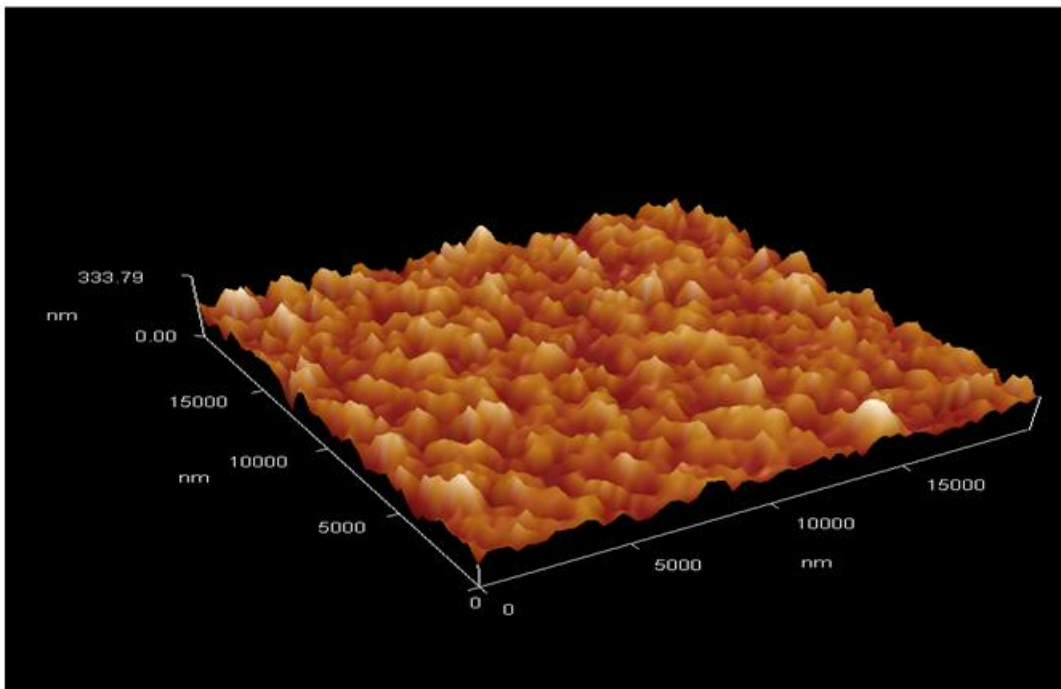


Figure 9. AFM image of ZnO nanofilm shows the surface morphology of the film deposited on quartz substrate

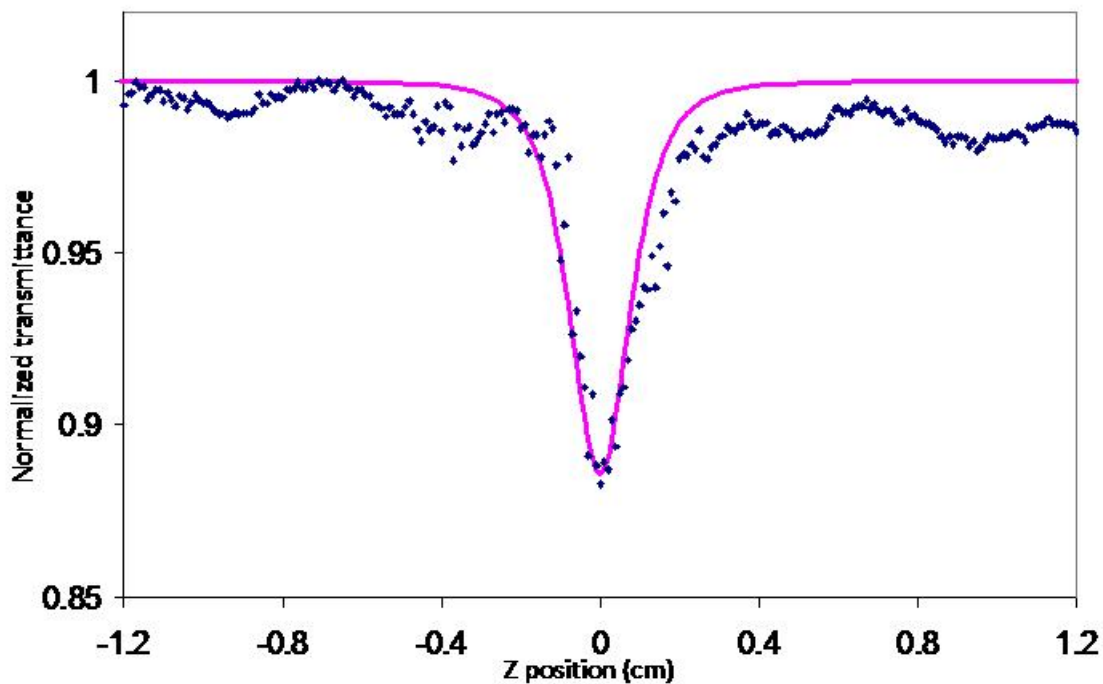


Figure 10. OA Z-scan measured at irradiance 79 GW/cm^2 , wavelength 800 nm, a pulse duration 60 fs and repetition rate of 250 kHz. The solid line is the fitting curve employing the Z-scan theory, described in the text, on 3PA

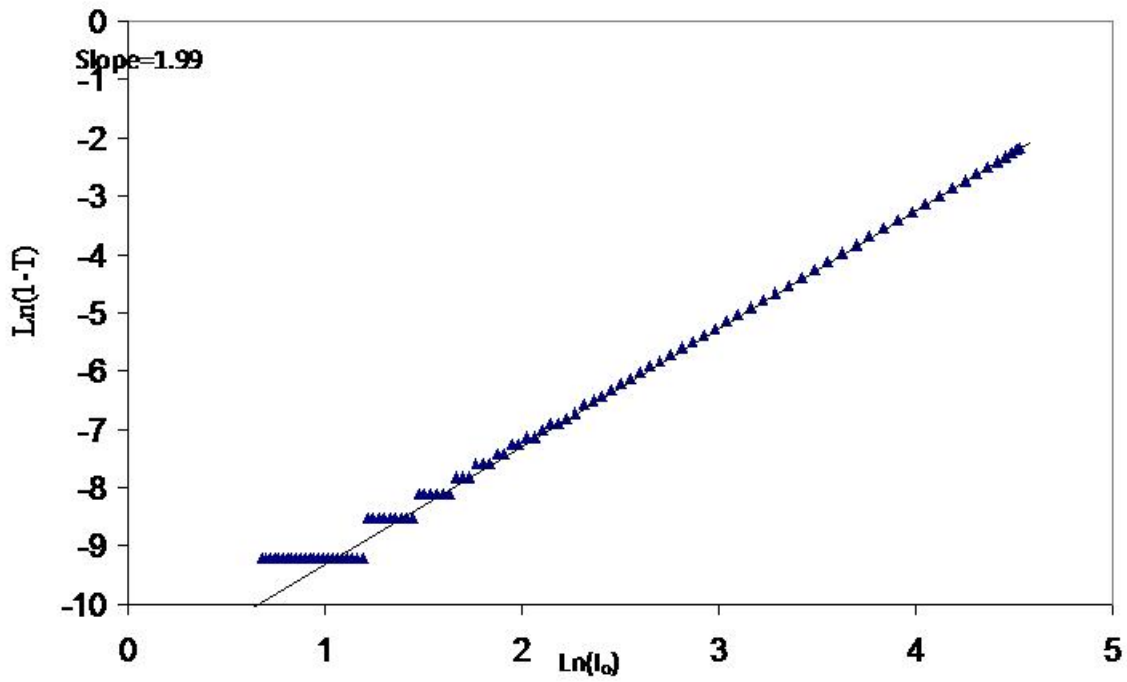


Figure 11. Plot of $\ln(1-T)$ versus $\ln(I_0)$ at 800nm wavelength, the solid line is the example of the linear at 800nm with slope $s=1.99$